*Planet. Space Sci.*, Vol. 39, No. 4, pp. 641–654, 1991
Printed in Great Britain.

0032-0633/91 $3.00 + 0.00
Pergamon Press plc

# METHODS FOR QUANTITATIVE MODELING OF THE MAGNETIC FIELD FROM BIRKELAND CURRENTS

N. A. TSYGANENKO
Institute of Physics, Leningrad University, Stary Petergof 198904, Leningrad, U.S.S.R.

(*Received* 29 *May* 1990)

**Abstract**—A quantitative model of the magnetic field from the large-scale system I of Birkeland currents in the Earth's magnetosphere is proposed. In the near-Earth space the electric current flow lines follow the dipolar magnetic field lines, while at larger distances they enter the high-latitude magnetosheath near mid-day, the low-latitude boundary layer along the magnetospheric flanks, and the plasma sheet boundary layer at the nightside. The model takes into account the local time dependence of the latitude of Birkeland current zone at the topside ionospheric level reported by Iijima and Potemra (1976, *J. geophys. Res.* **81,** 2165.) The effects of the geodipole tilt in the overall geometry of the field-aligned current system are also incorporated. The model is sufficiently flexible; in particular, it permits an arbitrary choice of the current sheet thickness as well as of the M.L.T. distribution of the current intensity by using an appropriate combination of model coefficients in the corresponding Fourier expansion. One more possibility is to take into account the asymmetry in the net intensity and M.L.T. distribution of Birkeland currents between Northern and Southern Hemispheres which arises due to diurnal and seasonal variations of the geodipole tilt angle. The proposed analytical representation is relatively simple, which allows it to be incorporated in semi-empirical statistical magnetospheric models with parameters to be determined from spacecraft databases.

Two other approaches to the modeling of warped current sheets aimed at quantitative approximation of the magnetic field of Birkeland and tail current systems are considered.

## 1. INTRODUCTION

Large-scale systems of field-aligned currents, of which the existence was first guessed by Birkeland (1908), were experimentally studied by Zmuda and Armstrong (1974) at heights of the topside ionosphere. More complete statistical investigations of the average distribution of the currents by using the data from the *TRIAD* (Iijima and Potemra, 1976a,b) and *MAGSAT* (Bythrow *et al.*, 1983) spacecraft also refer to comparatively low altitudes ($h < 1000$ km). As it concerns more distant magnetospheric regions, the experimental evidence for Birkeland currents is much more sparse. Nevertheless, the effects of crossing the layers of Birkeland currents by spacecraft are clearly discernible up to distances beyond 10 $R_E$, the results being in a good agreement with the expected overall geometry of the systems I and II (Sugiura, 1975, 1976; Kelly *et al.*, 1986).

According to the generally accepted view, the currents which belong to the mid-day part of system I are located on the field lines penetrating either the low-latitude boundary layer, or directly the magnetosheath (e.g. Saflekos *et al.*, 1982; Troshichev, 1982; Stern, 1983). The rest part of system I is most likely to be mapped into the tail region, being aligned there with the boundary layer plasma sheet. The low-latitude system II is connected with intra-magnetospheric sources, namely, with the Alfvén layer at the inner edge of the plasma sheet and probably with the partial ring current.

Even crude estimates of the net current flowing in the principal magnetospheric electric current circuits show that Birkeland currents must exert a strong influence upon the structure of the magnetospheric magnetic field. Indeed, according to the results of Iijima and Potemra (1976a), the net current flowing in systems I and II is on average about 2,000,000–3,000,000 Ampères in each hemisphere, and it is quite reasonable to expect values several times larger during extreme conditions. For comparison, the net current flowing at the dayside magnetopause across the noon meridian between the subsolar point and the polar cusp has the same order of magnitude (about 3,000,000 A); almost the same estimate can also be obtained for the total current flowing in the near part (up to $r \sim 15\ R_E$) of the tail plasma sheet and the ring current. Therefore, there is no doubt that an accurate account of Birkeland current systems should be considered as the prime task in quantitative modeling of the terrestrial and planetary magnetospheres. However, attempts to solve this problem meet with considerable difficulties.

## 2. GENERAL CONSIDERATIONS

One of the principal difficulties stems from lack of knowledge about the configuration of Birkeland

currents at large geocentric distances, where a relatively large contribution to the net magnetic field comes from extraterrestrial sources, including the field-aligned currents themselves. At closer distances ($r < 6$–$8\,R_E$) the field is quasi-dipolar; here the situation is clearer, since we know, at least approximately, the shape of the current flow lines [note, however, that even at the relatively close distances Rich *et al.* (1981) found significant inconsistencies in Birkeland current densities measured simultaneously at two different altitudes, which implies partial cross-**B** closure of the field-aligned currents between 300 and 3000 km]. This allows the evaluation of magnetic fields from the Birkeland current by specifying their local time distribution as obtained from the low-altitude measurements (see, e.g. Fig. 16 by Potemra in the review paper by Saflekos *et al.*, 1982) and then performing a numerical integration over the current sheets. Such calculations provide a quantitative evaluation of the magnetic effects produced by Birkeland currents at different locations (Sugiura, 1976; Tsyganenko and Suslikov, 1982). However, such "wire" models are almost useless for practical applications, since for evaluating the field components at any point of space it is necessary to integrate over the two-dimensional surface; in the vicinity of current layers there also arise troubles with singularities of the integrands in Biot–Savart integrals. The main drawback of this approach is that it only provides a solution of a direct problem in which the parameters of the current system are considered to be fixed at some *a priori* specified values. However, the most interesting and promising prospects in geophysical research are related to development of the inverse problem methods, in which parameters of the modeled object are derived by adjusting the model to fit experimental databases. This approach requires development of quantitative models of magnetospheric current systems with the following properties.

(i) A sufficient flexibility which is defined by the number of independent free parameters. From the computational point of view, it is desirable that the parameters be linear, to enable the entry of the model expressions as coefficients. On the other hand, it is also important that the parameters have clear physical meaning, such as, for example, the tail current sheet thickness or the subsolar point distance.

(ii) Mathematical simplicity of expressions and/or algorithms representing the model field distribution. This requirement becomes important if sufficiently large experimental databases are involved in the numerical fitting procedure.

(iii) The model representation should not contain any singularities or discontinuities of the magnetic field and must also satisfy the condition $\nabla \cdot \mathbf{B} = 0$.

It is worth noting in addition that the choice of mathematical methods for modeling should be done with an account of the most essential *a priori* information on the observed structure of the corresponding electric current system, in particular by using the data on charged particles.

The outlined approach to modeling magnetospheric current systems was developed in our earlier papers (Tsyganenko and Usmanov, 1982; Tsyganenko, 1987, 1989). However, neither of the proposed models incorporates in an explicit form the contribution from the field-aligned current systems, though their average effect is actually included in the group of terms representing the magnetic field of the magnetopause current. Recently, some attempts have been made to create more elaborate methods for modeling the field from Birkeland currents. Thus, Tsyganenko (1988) proposed an explicit model of the systems I and II magnetic field, based on a modification of the vector potential corresponding to a toroidal field. Stern (1989) proposed an interesting method for modeling system II, starting from a Euler potential representation for a purely dipolar magnetic field.

In the present work new methods pertaining to the modeling of the system I of Birkeland currents are proposed. System I is the most large-scale field-aligned current circuit extending from ionospheric heights up to the magnetospheric boundary and remote regions of the tail plasma sheet. It forms a natural transition layer dividing the whole magnetosphere into two domains with essentially different physical regimes of plasma and magnetic field topology (Sugiura, 1975, 1976): the polar cap region and the low-latitude magnetosphere (including the auroral region). Birkeland currents manifest themselves in an abrupt rotation of the field vector on crossing the current sheet. This effect is observed throughout the whole extension of the current "curtain". At low altitudes, however, the rotation of **B** must be smaller than at larger distances, in spite of which the absolute values of $\Delta\mathbf{B}$ across the sheet are much larger near the Earth (of the order of several hundreds of nanoteslas) due to the convergence of the electric current flow lines. An obvious reason is that the current density integrated over the layer thickness (proportional to $\Delta B$) decreases with the geocentric distance, roughly as $r^{-3/2}$, while the net $B$ magnitude falls off much more rapidly as $r^{-3}$.

In a crude approximation, the global distribution of the magnetic field **B** from the system I current is such that, at a fixed altitude, the **B** vector does not

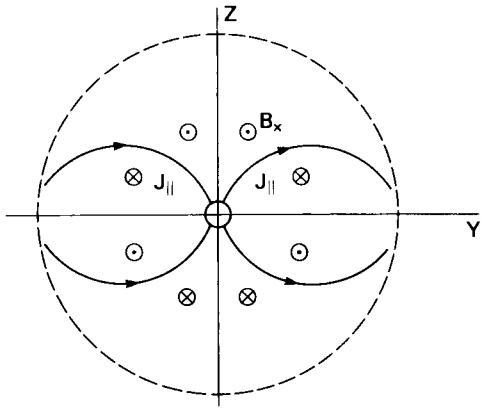


FIG. 1. ILLUSTRATING THE MAGNETIC EFFECT OF THE SYSTEM I OF BIRKELAND CURRENTS IN THE DAWN–DUSK MERIDIONAL CROSS-SECTION OF THE MAGNETOSPHERE.

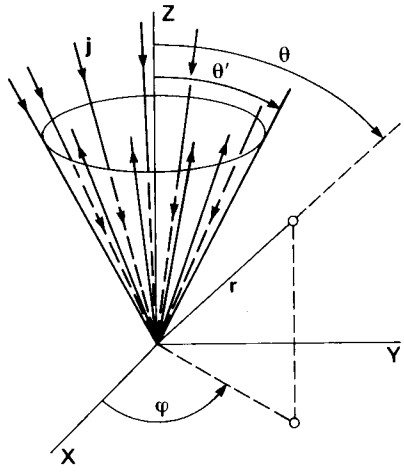


FIG. 2. THE INITIAL ELECTRIC CURRENT SYSTEM FOR THE CONICAL MODEL OF BIRKELAND CURRENTS.
The current is flowing radially to and from infinity, being confined within the infinitesimally thin conical current sheet.

change significantly in the polar cap regions, being directed sunward in the Northern Hemisphere and antisunward in the Southern. At low latitudes in the dawn–dusk sectors the field is directed oppositely to that in the adjacent polar cap and reverses its direction on crossing the equatorial region, as shown in Fig. 1. At the dayside the system I current induces a depression in the net $B$ which leads to an equatorial shift of polar cusps, most pronounced during disturbed periods. In the nightside magnetosphere the field-aligned currents are localized in the plasma sheet boundary layer and, most likely, are produced by a different physical mechanism than those in the daytime sector. For this reason it is desirable that the quantitative model be able to reproduce variations in the relative intensity of the currents flowing in the different M.L.T. sectors of the system I "curtain".

## 3. THE CONICAL MODEL OF SYSTEM I OF BIRKELAND CURRENTS

A general outline of the proposed method is as follows. First of all we derive expansions for the vector potential of the magnetic field produced by a distribution of electric current flowing along generatrices of the conical surface shown in Fig. 2. The derived potentials are then used for extending the result to the case of the conical current layer of a finite angular thickness. The last step is to introduce a deformation of the current layer, in order to simulate the expected overall configuration of system I. This is achieved by applying a transformation of coordinates entering the expansions for the corresponding vector potential. The resultant magnetic field $\mathbf{B} = \nabla \times \mathbf{A}$ remains divergenceless; this is one of advantages of the method, which closely resembles that used for constructing a model of the warped tail current sheet (Tsyganenko, 1989).

### 3.1. *Magnetic field from the conical current sheet*

Let us introduce a spherical coordinate system $(r, \theta, \varphi)$ and assume that the vector potential corresponding to the conical current sheet shown in Fig. 2 has the only radial component $A_r \equiv A(r, \theta, \varphi)$. The magnetic field components are

$$B_r = 0, \quad B_\theta = \frac{1}{r \sin\theta} \frac{\partial A}{\partial \varphi}, \quad B_\varphi = -\frac{1}{r} \frac{\partial A}{\partial \varphi}. \quad (1)$$

The electric current density is

$$\mathbf{j} = (c/4\pi) \nabla \times \nabla \times \mathbf{A}, \quad (2)$$

and, since we assume $j_\theta = j_\varphi = 0$, it follows that

$$\frac{\partial^2 A}{\partial r \, \partial \theta} = 0 \quad \text{and} \quad \frac{\partial^2 A}{\partial r \, \partial \varphi} = 0,$$

and hence that $\partial A / \partial r = 0$, or $A = A(\theta, \varphi)$.

The radial component of the electric current should vary with distance as $r^{-2}$, in order to ensure the continuity condition $\nabla \cdot \mathbf{j} = 0$, and can be specified as a given function of the azimuthal angle represented by Fourier series, so that we can treat the problem for each term separately.

Assuming now the system I current to be symmetric with respect to the noon–midnight meridian plane (this assumption is not essential and the foregoing

treatment can be readily generalized for a non-symmetric case), we have for the $m$th term

$$j_r^{(m)} = \frac{\sin m\varphi}{r^2}\delta(\theta-\theta'), \tag{3}$$

where $\theta'$ is the angular half-width of the cone and the weight coefficient is taken to be unity for simplicity. Separating the variables in the vector potential as

$$A^{(m)} = T^{(m)}(\theta)\sin m\varphi \tag{4}$$

and writing down the radial component of Ampère's law (2), we obtain

$$\hat{L}_m T^{(m)} \equiv \frac{\partial^2 T^{(m)}}{\partial\theta^2} + \cot\theta\frac{\partial T^{(m)}}{\partial\theta} - \frac{m^2}{\sin^2\theta}T^{(m)} = \delta(\theta-\theta'). \tag{5}$$

Solution of equation (5) provides Green's function $G^{(m)}(\theta,\theta')$ which enables us to solve a more general problem

$$\hat{L}_m T^{(m)} = F(\theta) \tag{6}$$

in particular, to find the vector potential corresponding to a conical current layer with a finite angular thickness contained within the interval $\theta^- < \theta < \theta^+$. In the last case $F(\theta) \neq 0$ inside the interval and is zero outside of it. The solution is given by the integral

$$T^{(m)}(\theta) = \int_{\theta^-}^{\theta^+} G^{(m)}(\theta,\theta')F(\theta')\,d\theta'. \tag{7}$$

To obtain $G^{(m)}(\theta,\theta')$, we have first to derive two independent solutions of the corresponding uniform equation

$$\hat{L}_m T^{(m)} = 0.$$

These are (Kamke, 1959, formula 2.370).

$$T_1^{(m)}(\theta) = \tan^m\frac{\theta}{2} \quad \text{and} \quad T_2^{(m)}(\theta) = \cot^m\frac{\theta}{2}. \tag{8}$$

In principle, the function $G^{(m)}(\theta,\theta')$ can be obtained from (8) by using a standard method (e.g. Korn and Korn, 1968, ff. 9.3–7 and 9.3–9). However, in our case it is more convenient to use another approach, taking into account that the currents are flowing inside a relatively thin layer. Namely, let us consider

$$G^{(m)}(\theta,\theta') = T_1^{(m)}(\theta)[1-H(\theta-\theta')] + T_2^{(m)}(\theta)H(\theta-\theta')\cdot C(\theta'), \tag{9}$$

where $H$ is Heaviside step function, defined as $H(x) = 0$ for $x < 0$ and $H(x) = 1$ for $x > 0$. The function $C(\theta')$ is introduced in order to ensure continuity of Green's function (8) with respect to $\theta$ at $\theta = \theta'$. This requires

$$C(\theta') = T_1^{(m)}(\theta')/T_2^{(m)}(\theta'). \tag{10}$$

It can be shown that substitution of (9) and (10) in (7) yields a function $T_*^{(m)}(0)$ which, being inserted under the differential operator $\hat{L}_m$ in (6), leads to the result

$$\hat{L}_m T_*^{(m)}(\theta) = F(\theta)\cdot 3W^{(m)}(\theta)/T_2^{(m)}(\theta), \tag{11}$$

rather than $F(\theta)$, as required by (6). Here $W^{(m)}$ is the Wronskian composed of the solutions $T_1^{(m)}$ and $T_2^{(m)}$. Nevertheless, in our particular case this inconsistency does not matter, since the function $F(\theta)$ is zero everywhere except a narrow interval of $\theta$ and the additional factor in (11) can be accounted for merely by an appropriate renormalization of coefficients. On the other hand, standard methods for derivation of Green's function turn out to lead to more complex final expressions and that is why we have chosen it in the form (9).

From equations (7) and (9) we have

$$T^{(m)}(\theta) = T_1^{(m)}(\theta)\int_{\theta^*}^{\theta^+} F(\theta')\,d\theta' + T_2^{(m)}(\theta)\int_{\theta^-}^{\theta^*} C(\theta')F(\theta')\,d\theta', \tag{12}$$

where

$$\theta^* = \begin{cases} \theta^- & \text{for} \quad \theta < \theta^- \\ \theta & \text{for} \quad \theta^- < \theta < \theta^+ \\ \theta^+ & \text{for} \quad \theta > \theta^+. \end{cases}$$

Which analytic form should be chosen for the function $F$ defining the electric current profile? At first glance, the rectilinear "impulse" profile would seem the simplest choice. However, this leads to somewhat cumbersome quadratures in the second integral in (12). On taking account of (8) a much more convenient form for $F(\theta)$ is found to be that containing the derivative of $\tan\theta/2$ as a factor. This slightly modifies the slope of the current density profile across the layer (see Figs 4–6 below) and does not exert any significant influence on the overall magnetic field distribution. Bearing in mind the subsequent deformation of the conical current surface, we introduce a normalization factor, in order to keep the net current flowing between $\theta^-$ and $\theta^+$ at different geocentric distances constant. All these considerations lead to:

$$F(\theta') = \begin{cases} \dfrac{1}{2\cos^2\dfrac{\theta'}{2}\left(\tan\dfrac{\theta^+}{2}-\tan\dfrac{\theta^-}{2}\right)} \\ \quad \text{for} \quad \theta^- < \theta' < \theta^+ \\ 0 \quad \text{for} \quad \theta' < \theta^- \quad \text{or} \quad \theta' > \theta^+. \end{cases} \tag{13}$$

Substituting (13) in (12) yields

$$T^{(m)}(\theta) = \begin{cases} \tan^m\dfrac{\theta}{2} \quad \text{for } \theta < \theta^- \\ \dfrac{1}{\tan\dfrac{\theta^+}{2}-\tan\dfrac{\theta^-}{2}}\left[\tan^m\dfrac{\theta}{2}\left(\tan\dfrac{\theta^+}{2}-\tan\dfrac{\theta}{2}\right)\right. \\ \left. + \dfrac{\tan^{2m+1}\dfrac{\theta}{2}-\tan^{2m+1}\dfrac{\theta^-}{2}}{(2m+1)\tan^m\dfrac{\theta}{2}}\right] \\ \quad \text{for} \quad \theta^- < \theta < \theta^+ \\ \dfrac{\tan^{2m+1}\dfrac{\theta^+}{2}-\tan^{2m+1}\dfrac{\theta^-}{2}}{(2m+1)\left(\tan\dfrac{\theta^+}{2}-\tan\dfrac{\theta^-}{2}\right)}\cot^m\dfrac{\theta}{2} \\ \quad \text{for} \quad \theta > \theta^+. \end{cases} \tag{14}$$

On being substituted in (4) $T^{(m)}(\theta)$ yields the $m$th term of the vector potential expansion which, with a proper choice of coefficients, can in principle represent the field produced by an arbitrary azimuthal distribution of radial currents flowing within a thin conical current layer. Outside the layer the field is current-free, which can be verified by a direct substitution of the vector potential in (2).

### 3.2. *Deformation of the conical current layer*

The simplest way to make the necessary deformation of the conical current layer is to introduce the dependence of the parameters $\theta^-$ and $\theta^+$ in (14) on $r$ and $\varphi$. In such a case at different distances and azimuthal angles the current sheet crossings will be observed at different values of $\theta$. It is more convenient now to introduce parameters $\theta_0$ and $\Delta\theta$ instead of $\theta^+$ and $\theta^-$, so that $\theta^+ = \theta_0 + \Delta\theta$ and $\theta^- = \theta_0 - \Delta\theta$. The shape of the Birkeland current sheet is defined by the choice of the function $\theta_0 = \theta_0(r, \varphi)$. In principle, the angular half-thickness of the current sheet, $\Delta\theta$, can also be made to depend on $r$ and $\varphi$. Thus defined deformation of the current sheet brings some modification in the expressions for the magnetic field components which, for the $m$th terms of the expansions, are now

$$B_r^{(m)} = 0$$

$$B_\theta^{(m)} = \frac{1}{r\sin\theta}\left(mT^{(m)}\cos m\varphi + \frac{\partial T^{(m)}}{\partial\theta_0}\frac{\partial\theta_0}{\partial\varphi}\sin m\varphi\right)$$

$$B_\varphi^{(m)} = -\frac{1}{r}\frac{\partial T^{(m)}}{\partial\theta}\sin m\varphi. \tag{15}$$

How does one define the function $\theta_0(r, \varphi)$? It is evident that, for small geocentric distances, $\theta_0$ and $r$ must satisfy the dipolar field line equation $r = L\sin^2\theta_0$. The $L$ parameter must depend on the local magnetic time in such a way that in the daytime sector the field-aligned current sheet be mapped onto the ionosphere at latitudes 78–80° and to descend equatorward up to 70–72° at the nightside, in line with the results of Iijima and Potemra (1976a). At larger distances, that is for $r > L$, it is natural to impose a requirement on $\theta_0(r, \varphi)$ to approach asymptotic values near 90°, so that in the noon, dawn and dusk sectors the outer edge of the current layer be immersed into the low-latitude boundary layer, and in the nightside magnetosphere the current flow lines be aligned with the plasma sheet boundary layer. These requirements are met by choosing the following relationships between $r$, $\theta_0$, and $\varphi$

$$\sin^2\theta_0 = \frac{1}{2L}\left[\sqrt{(r+L)^2+\delta^2} - \sqrt{(r-L)^2+\delta^2}\right]$$

$$L = L(\varphi) = L_1 + L_2\cos\varphi, \tag{16}$$

where the parameters $L_1$ and $L_2$ yield the location and shape of the zone I of Birkeland currents and $\delta$ defines the degree of abruptness of the transition from the quasi-dipolar shape of the current flow lines at $r < L$ to that stretched parallel to the dipole equator at $r > L$.

The next feature to be taken into account is the influence of the geodipole tilt upon the shape of the current layer. To our knowledge, this effect has not been studied experimentally so far; nevetheless, there exist weighty indirect considerations concerning this point. Indeed, it is natural to suggest that in the noon sector the location of the system I current is closely related to that of the polar cusps. The latter can be assumed in a crude approximation to be rigidly tied to the geodipole axis orientation and hence be fixed in the solar-magnetic coordinate system. In a more accurate treatment a latitudinal shift of the cusps

toward summer polar cap (not larger than by 3–4° for maximal tilt angles of $\psi \approx \pm 35°$) should be taken into account, following the results of model calculations (e.g. Mead and Fairfield, 1975; Tsyganenko, 1990) and spacecraft measurements (Newell and Meng, 1989). At the nightside it is natural to model the tilt-related deformation of the system I current layer in accordance with the observed warping of the tail plasma sheet, assuming that for $r < L$ the attitude of the Birkeland current layer is also approximately fixed in the solar-magnetic coordinate system.

Taking into account all these considerations, we choose the function $\theta_{0n}$ for approximating the Birkeland current layer geometry in the northern hemisphere as

$$\theta_{0n}(r, \varphi, \psi) = \arcsin\left\{\frac{1}{2L}\left[\sqrt{(r+L)^2+\delta^2}-\sqrt{(r-L)^2+\delta^2}\right]\right\}^{1/2} - \frac{1}{2r}\left[\sqrt{(r-L)^2+\delta^2}+r-L\right]\psi\cos\varphi. \quad (17)$$

The first term corresponds to (16) and yields the shape of the current sheet for the perpendicular geodipole orientation. The second term accounts for the dipole tilt effects and, in line with the above arguments, becomes significant only for $r > L$. If necessary, this approximation can be improved by introducing the tilt-related effects in the inner magnetosphere as well. This can be done, for example, by means of the following modification of the second term in (17)

$$-\frac{1}{2r}\left\{\left[\sqrt{(r-L)^2+\delta^2}+r-L\right]+f(r,\varphi)\right\}\psi\cos\varphi,$$

where $f(r, \varphi)$ is a relatively small quantity which models more detailed effects of the diurnal and seasonal variations of the position of the polar cap boundary at middle and low altitudes.

In the Southern Hemisphere the shift of the current layer due to the dipole tilt must be nearly the reverse of that in the Northern Hemisphere and, hence, the opposite sign should be ascribed to the second term in (17) in this case.

In Fig. 3 the shape of the northern and southern Birkeland current layer represented by (17) is shown in the noon–midnight and dawn–dusk cross-sections for the maximal value of the tilt angle $\psi = 34°$ and with: $L_1 = 15R_E$, $L_2 = 5R_E$, and $\delta = 2R_E$.

### 3.3. *Derivation of the net magnetic field components*

The net model magnetic field is composed of contributions coming from the northern and southern current layers. Note first of all that in a limited range

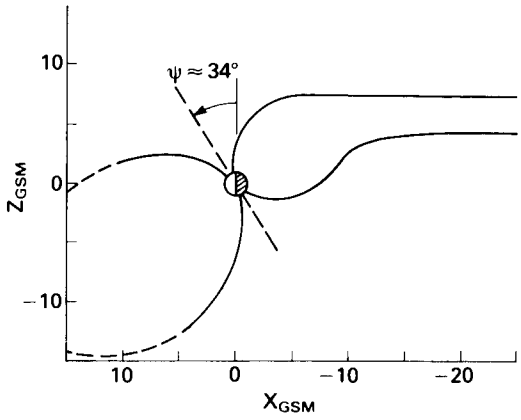


FIG. 3a. NOON–MIDNIGHT CROSS-SECTION OF THE SURFACE (17) DEFINING THE WARPED CURRENT LAYER IN THE MODEL SYSTEM I OF BIRKELAND CURRENTS, FOR $\psi = 34°$.

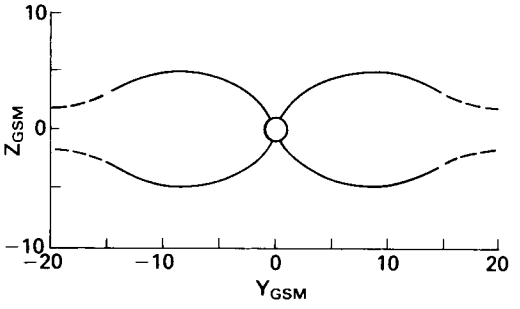


FIG. 3b. DAWN–DUSK CROSS-SECTION OF THE MODEL SURFACE (17).

of altitudes just above the ionosphere ($h < 0.5R_E$) the model is likely to be inaccurate, since the currents are closing in the vicinity of the origin, rather than via the ionosphere, as is really the case. It should be realized, however, that the degree of the inconsistency depends on the degree of non-uniformity of the ionospheric conductivity. In an ideal case of a completely uniform conductivity distribution it can be shown by using the same arguments as those given in the proof of Fukushima's theorem (Fukushima, 1969), that above the ionosphere the contribution from the Pedersen current closing each Birkeland current "wire" is nearly equivalent to the field produced by a rectilinear current segment connecting the ionospheric end of the "wire" with the origin, i.e. just as in the present model.

The next important point is that the intensities of Birkeland currents in the summer and winter hemispheres can considerably differ from each other, due

to asymmetry of the conductivity distribution for $\psi \neq 0$ (Fujii *et al.*, 1981). In the proposed model this can be easily taken into account by representing the Fourier coefficients in the vector potential expansions for each half of the entire current system as a sum of two terms, of which the first one is symmetrical and the second is antisymmetrical with respect to the tilt angle $\psi$.

Having made these comments, we give the final expansions for calculating the magnetic field components. The contribution from the northern half of the model current system is represented in the spherical solar-magnetic coordinates by the sum of $M$ leading terms:

$$B_{\theta n} = \frac{1}{r \sin\theta} \sum_{m=1}^{M} (a_m \cos\psi + b_m \sin\psi) \times \left( m T_n^{(m)} \cos m\varphi + \frac{\partial T_n^{(m)}}{\partial \theta_{0n}} \frac{\partial \theta_{0n}}{\partial \varphi} \sin m\varphi \right)$$

$$B_{\varphi n} = -\frac{1}{r} \sum_{m=1}^{M} (a_m \cos\psi + b_m \sin\psi) \frac{\partial T_n^{(m)}}{\partial \theta} \sin m\varphi, \quad (18)$$

where the functions $T_n^{(m)}$, their derivatives $\partial T_n^{(m)}/\partial\theta$ and $\partial T_n^{(m)}/\partial\theta_{0n}$, and also $\partial\theta_{0n}/\partial\varphi$ can be obtained in a straightforward way from (14) and (17); the index n means that the quantities refer to the northern current layer. Similar expressions for the southern layer are:

$$B_{\theta s} = \frac{1}{r \sin\theta} \sum_{m=1}^{M} (a_m \cos\psi - b_m \sin\psi) \times \left( m T_s^{(m)} \cos m\varphi + \frac{\partial T_s^{(m)}}{\partial \theta_{0s}} \frac{\partial \theta_{0s}}{\partial \varphi} \sin m\varphi \right)$$

$$B_{\varphi s} = \frac{1}{r} \sum_{m=1}^{M} (a_m \cos\psi - b_m \sin\psi) \frac{\partial T_s^{(m)}}{\partial \theta_{0s}} \sin m\varphi. \quad (19)$$

Calculation of the functions $T_s^{(m)}$, their derivatives, and $\partial\theta_{0s}/\partial\varphi$ should be done by using equations (14) and (17), the differences being that (i) $\tan\theta/2$ in (14) is to be replaced by $\cot\theta/2$ and vice versa, and (ii) the sign of the second term in (17) should be plus instead of minus.

Figures 4–6 show the results of computation of the profiles of the volume current density and the magnetic field components along the lines crossing the field-aligned current layer in the dayside, dawn–dusk, and nightside sectors. As can be seen from the plots, the results obtained are close to those expected from the *a priori* considerations discussed in Section 2. As a consequence of the transformation distorting the initially conical shape of the current surface, a secondary electric current arises outside the warped layer. This defect is an inevitable artifact of the method of the vector potential modification. However, the volume density of the secondary currents is on average much smaller than that inside the model Birkeland current layer and the corresponding

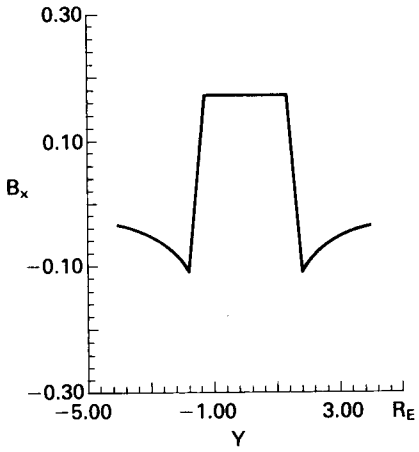


FIG. 4a. PLOT OF $B_x$ IN THE MODEL OF BIRKELAND CURRENT SYSTEM, COMPUTED ALONG THE LINE $x = 0.2R_E$, $z = 3R_E$, PARALLEL TO THE $Y$ AXIS, THAT IS ACROSS THE POLAR CAP REGION.
The field is nearly uniform in the $X$ and $Y$ directions throughout the polar cap and displays abrupt reversals on crossing the model field-aligned current layers, with downward and upward current at dawn and dusk, respectively.

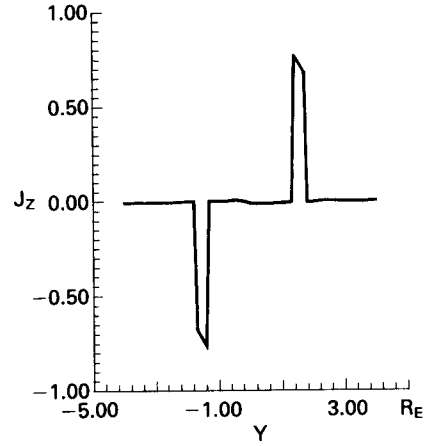


FIG. 4b. PLOT OF THE $Z$-COMPONENT OF THE VOLUME CURRENT DENSITY CORRESPONDING TO THE $B_x$ PLOT IN FIG. 4a.
Note a non-constancy of $j$ inside the layers (see text for explanation).

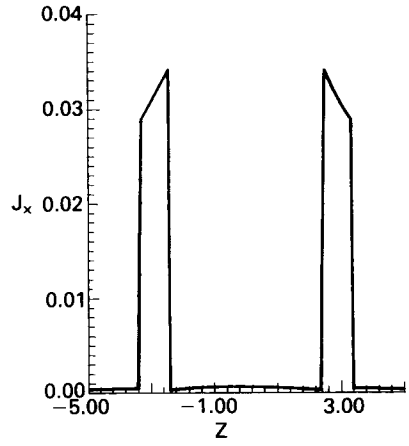


FIG. 5. PLOT OF $j_x$ ALONG THE LINE $x = -10R_E$, $y = -2R_E$, PARALLEL TO THE $Z$-AXIS, THAT IS ACROSS THE PLASMA SHEET IN THE NEAR TAIL REGION.
The profile crosses the northern and southern layers with sunward Birkeland currents.

magnetic field should have a much larger variation scale, so that in principle it can be eliminated by introducing simple polynomial terms in the modeling expressions. Note also that the current density profiles across the layer are not flat. This is a consequence of the adopted method of defining Green's function (9) as well as of the "turning inside out" deformation of the initial conical current layer.

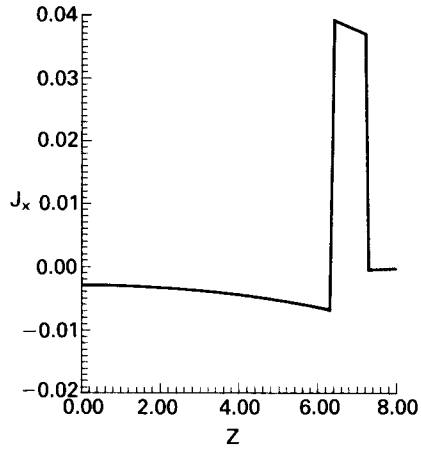


FIG. 6a. PLOT OF $j_x$ ALONG THE LINE $x = 6R_E$, $y = 2R_E$, PARALLEL TO THE $z$ AXIS, THAT IS ACROSS THE DAYSIDE CUSP REGION.
The model Birkeland current layer is located at $6R_E < z < 8R_E$. Note a significant secondary current density in the low-latitude region $z < 6R_E$.

Figure 7 illustrates the overall distribution of the **j** vector inside the model current layer in projection onto the plane $z = 0$. It displays a family of unit vectors $\mathbf{h} = (\mathbf{j}_x + \mathbf{j}_y)/(j_x^2 + j_y^2)^{1/2}$ showing at each point the direction of the electric current component parallel to the equatorial plane. Note that the vectors in the figure are not strictly radial and there exist two wedge-shaped regions centered about the $x$-axis with the current flow lines crossing the noon–midnight meridian plane, while in the initial conical model (Fig. 2) all the lines pass through the cone vertex. This is the artifact of the imposed deformation; however, this does not seem to be a serious drawback for the following reasons: (i) the net current crossing the noon–

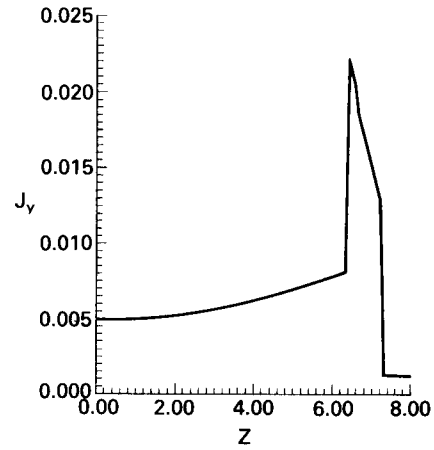


FIG. 6b. SAME AS FIG. 6a, EXCEPT FOR THE $j_y$ COMPONENT.

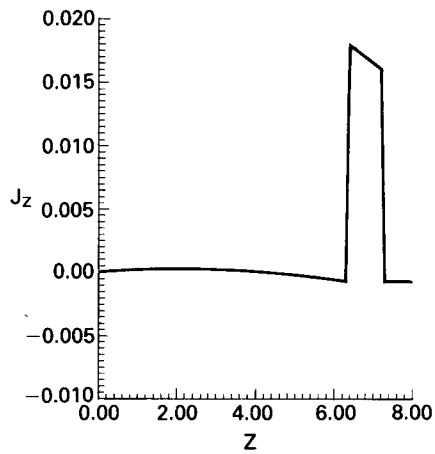


FIG. 6c. SAME AS FIG. 6a, EXCEPT FOR THE $j_z$ COMPONENT.

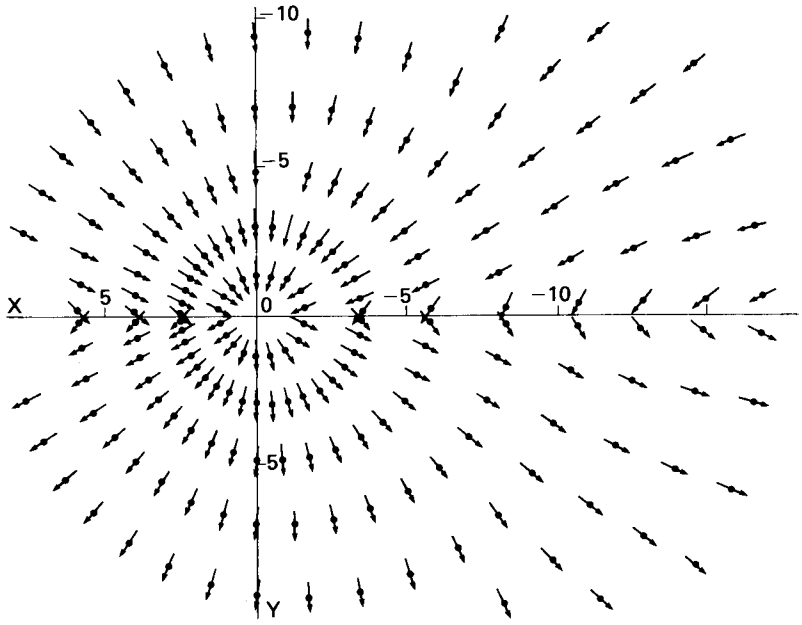


FIG. 7. EQUATORIAL PROJECTIONS OF THE ELECTRIC CURRENT DENSITY VECTORS COMPUTED INSIDE THE MODEL BIRKELAND CURRENT LAYER.
Due to normalization, all the vectors are of equal length, thus showing only directions of the electric current in projection onto the plane $z = 0$. Note that a small portion of the net current crosses the noon–midnight meridian plane at relatively large distances, in contrast with the corresponding electric current pattern in the initial conical model of Fig. 2 (see text).

midnight plane outside the Earth is relatively small; and (ii) both in the noon and midnight sectors the secondary azimuthal currents coincide in direction with the diamagnetic currents flowing at the equatorward boundary of the polar cusp and in the plasma sheet boundary layer.

### 3.4. *Modeling the effects of interhemispherical field-aligned current*

One more possibility of the proposed approach should also be pointed out. In the above outlined derivation of the $m$th term of the expansion for the vector potential we have not included the one with $m = 0$, because it corresponds to radial currents which do not depend on the local time. This means that there exists a source or a sink of the electric current at the cone vertex and, hence, the solution is physically senseless if we consider only half of the current system. However, the current inflow in, say, the Northern Hemisphere can be balanced by the corresponding outflow in the Southern one. From this follows the possibility of modeling a hypothetical effect of interhemispherical electric current flow related to the IMF $B_y$-component (Leontyev and Lyatsky, 1974).

For this case, having integrated the uniform equation corresponding to (4) with $m = 0$, we obtain the solutions,

$$T_1^{(0)} = \text{constant} \quad \text{and} \quad T_2^{(0)} = \ln \tan \theta/2, \quad (20)$$

where the first one refers to the polar cap regions (inside the conical cavities) and the second refers to the low-latitude region. The corresponding magnetic field is zero inside the cones and has the only azimuthal component $B_\varphi \sim (r \cdot \sin \theta)^{-1}$ outside. This result is also evident from simple considerations taking into account the axial symmetry and Ampère's law in its integral form. The potentials (20) can be used in a similar way for constructing the warped Birkeland current layer model. Introducing the corresponding terms in the magnetic field representation yields a dawn–dusk asymmetry whose sign and degree depend on the IMF orientation. This opens the possibility of studying these effects on a statistical basis by fitting the corresponding model parameters to the spacecraft datasets.

The dawn–dusk asymmetry of the magnetic field can also be induced by a prevalence of Birkeland currents inflow (outflow) at the dayside, with a corresponding outflow (inflow) at the nightside in the same hemisphere (Crooker and Siscoe, 1981; Suzuki and Fukushima, 1984). Such an asymmetry can be modeled by including in the expansions (18) and (19) the terms containing $\cos m\varphi$ ($-\sin m\varphi$) instead of $\sin m\varphi$ ($\cos m\varphi$), as has already been mentioned briefly in Section 3.1.

## 4. MODELS BASED ON DEFORMATION OF INITIALLY FLAT CURRENT SHEETS

The conical current sheet described in Section 3.1 seems to be the best generic surface for global modeling of system I of the Birkeland currents by using the method of vector potential modification. In local modeling studies two other models can also be applied. These are based on planar current sheets with a sufficiently flexible distribution of the electrical current density. The models outlined below can also be employed for a more refined quantitative simulation of the tail current system, including local transient redistributions of the current density in the near plasma sheet during substorms.

### 4.1. *A modification of the Tsyganenko–Usmanov current sheet model*

In one of our earlier papers (Tsyganenko and Usmanov, 1982) a simple method for modeling the tail current sheet was proposed, in which the current sheet is composed of continuously distributed spread-out straight current filaments. Each filament contributes the magnetic field $dB \sim \rho/(\rho^2+D^2)$, where $\rho$ is the distance from the central axis and $D$ is the characteristic half-thickness of the filament. Having chosen simple approximations for the electric current distribution along the sheet, it is possible to reduce the corresponding integrals to concise analytic expressions for the magnetic field components which satisfy the condition $\nabla\cdot\mathbf{B}=0$ and do not contain any singularities or discontinuities.

It is easy to generalize this model by introducing the effects of warping of the current sheet as well as variations of its thickness and width along the direction of current flow. Let the initial current sheet have the parameters $x_1$, $x_2$ and $x_m$, which define the location of its front and rear edges and of the current density maximum, respectively, as sketched in Fig. 8. If the current density profile along the sheet $J(x)$ has a triangular shape, then the expressions for the magnetic field components are

$$B_x = \frac{B_m}{2\pi} z \left\{ \frac{L_1}{\Delta x_1} + \frac{L_2}{\Delta x_2} + \frac{2}{\beta} \times \left[ S_1 A_1 + S_2 A_2 - (x-x_m) R \arctan \frac{x-x_m}{\beta} \right] \right\}$$

$$B_y = 0$$

$$B_z = \frac{B_m}{2\pi} \left\{ (x-x_m) \left( \frac{L_1}{\Delta x_1} + \frac{L_2}{\Delta x_2} \right) + L_2 - L_1 + 2\beta \left[ R \arctan \frac{x-x_m}{\beta} - \frac{A_1}{\Delta x_1} - \frac{A_2}{\Delta x_2} \right] \right\}, \quad (21)$$

where

$$B_m = 2\pi J(x_m)/c, \quad \beta^2 = z^2 + D^2,$$

$$\Delta x_1 = x_1 - x_m, \quad \Delta x_2 = x_m - x_2,$$

$$L_1 = \ln \frac{(x-x_m)^2+\beta^2}{(x-x_1)^2+\beta^2}, \quad L_2 = \ln \frac{(x-x_m)^2+\beta^2}{(x-x_2)^2+\beta^2},$$

$$S_1 = \frac{x-x_1}{\Delta x_1}, \quad S_2 = \frac{x-x_2}{\Delta x_2}, \quad A_1 = \arctan S_1,$$

$$A_2 = \arctan S_2, \quad R = \frac{1}{\Delta x_1} + \frac{1}{\Delta x_2}. \quad (22)$$

Now let the parameters $\Delta x_1$, $\Delta x_2$, $x_m$, and $D$ depend on $y$ and replace the coordinate $z$ by $z-z_s(y)$, where $z_s$ is a function defining the shape of the warped current layer. Such a modification does not violate the condition $\nabla\cdot\mathbf{B}=0$ and can yield the necessary shape of the model electric current flow lines. On the other hand, the modification again gives rise to the secondary currents outside the current sheet, the magnitude of which depends on the rate of the spatial variation of the model parameters.

### 4.2. *A generalization of the equatorial current disc model*

The recent version of our magnetospheric magnetic field model (Tsyganenko, 1989) was based on a model of the equatorial current disc which incorporated the warping effects due to the geodipole tilt. The model used a simple representation for the vector potentials corresponding to spread-out current discs with different rates of decrease of the electric current density with radial distance $\rho$ from the axis of symmetry.

As shown below, this approach can be extended to another class of models which provide a sector-shaped distribution of radial and azimuthal components of the electric current density. An appropriate modification of the $z$ coordinate provides a way to intro-

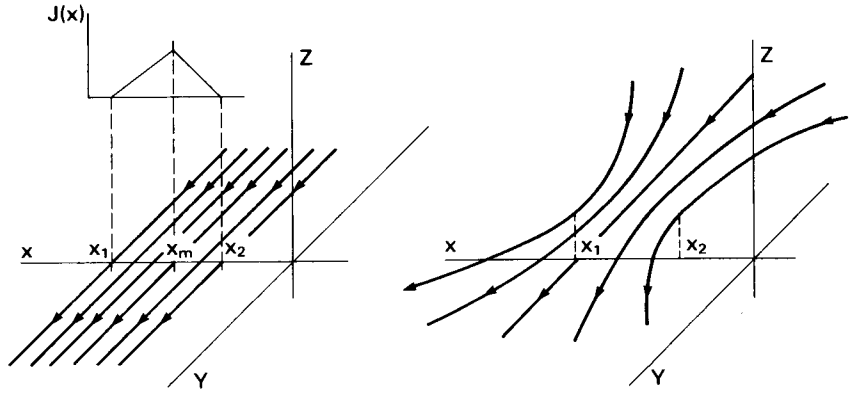


FIG. 8. A SKETCH OF THE INITIAL (LEFT) AND FINAL (RIGHT) CONFIGURATIONS OF THE SPREAD-OUT CURRENT SHEET WITH A TRIANGULAR PROFILE OF THE ELECTRIC CURRENT DENSITY, BASED ON THE MODEL OF TSYGANENKO AND USMANOV (1982).

duce a moderate warping of the initially flat sheets, which makes it possible to propose a further method for modeling the magnetic effects of Birkeland currents as well as for improving the tail field models.

The initial point for the present treatment is an infinitesimally thin current sheet in the equatorial plane $z = 0$ of the cylindrical coordinate system $(\rho, \varphi, z)$. Outside the current sheet the magnetic field is curl-free and hence can be represented by the gradient of a scalar potential which, in its turn, can be expanded in a series of cylindrical harmonics (e.g. Stern, 1987) with the $m$th term

$$\begin{Bmatrix}\cos m\varphi \\ \sin m\varphi\end{Bmatrix} \exp(\pm kz) J_m(k\rho), \tag{23}$$

where $J_m(k\rho)$ are Bessel functions of $m$th order.

In the case of the current disc (Tsyganenko, 1989) the situation was much easier due to the axial symmetry, which enabled us to represent the field by only the azimuthal component $A_\varphi$ containing the harmonics (23) with $m = 0$. We now consider a more general case, in which the radial component of **j** and the azimuthal component of **B**, varying with $\varphi$, are also present. It is evident that in the present case we cannot proceed with only one component of **A** and, hence, inevitably we arrive at a system of partial differential equations. To avoid this, let us choose another way, namely, consider first the scalar potential $u(\rho, \varphi, z)$. In the region $z > 0$ the $m$th harmonic can be represented as

$$u^{(m)} = \cos m\varphi \int_0^\infty C(k) \exp(-kz) J_m(k\rho)\, \mathrm{d}k. \tag{24}$$

The boundary condition for $u^{(m)}$ will be given by specifying the radial distribution of $B_z$ in the equatorial plane for $\varphi = 0$:

$$-\left.\frac{\partial u}{\partial z}\right|_{z=0,\varphi=0} = B_z(\rho) = \int_0^\infty kC(k) J_m(k\rho)\, \mathrm{d}k.$$

Inverting the last equation (Bateman and Erdelyi, 1954), we have

$$C(k) = \int_0^\infty B_z(\rho) J_m(k\rho)\rho\, \mathrm{d}\rho.$$

Since our goal is to obtain a representation for Birkeland current contribution which is the largest near the Earth due to convergence of the current flow lines, we choose the simplest dependence for $B_z(\rho)$ satisfying this criterion, namely, $B_z(\rho) \sim \rho^{-1}$. In this case $C(k) \sim k^{-1}$ and therefore (Bateman and Erdelyi, 1954)

$$u^{(m)} = \cos m\varphi \frac{[\sqrt{z^2+\rho^2} - z]^m}{\rho^m}. \tag{25}$$

Now we have to find a representation for the vector potential providing the same magnetic field as the scalar potential (25). This can be done by using a relation given by Stern (1987):

$$\mathbf{A} = \rho^2 \nabla\psi \times \nabla\varphi = \rho \nabla\psi \times \mathbf{e}_\varphi,$$

where $\psi$ is a scalar function related with the potential $u$ by the equation $u = -\partial\psi/\partial\varphi$. Using these relations, we obtain the components of the vector potential

$$A_\rho^{(m)} = -\sin m\varphi \frac{[\sqrt{1+z^2/\rho^2}-z/\rho]^m}{\sqrt{1+z^2/\rho^2}}$$
$$A_\varphi^{(m)} = 0, \quad A_z^{(m)} = A_\rho^{(m)} \cdot (z/\rho). \tag{26}$$

It can be verified by direct inspection that the vector potential (26) yields a curl-free magnetic field everywhere, while we need a current layer centered about the equatorial plane. It is found, however, that the vector potential corresponding to a current sheet with a half-thickness scale $D$ can be readily obtained from (26) by replacing $z$ with $\sqrt{z^2+D^2}$ in the expression for $A_\rho^{(m)}$. Rewriting (26) for the modified vector potential, we have finally

$$A_\rho^{(m)} = C^{(m)} \sin m\varphi \frac{\rho^{m+1}}{[\sqrt{\rho^2+\zeta^2}+\zeta]^m \sqrt{\rho^2+\zeta^2}}$$
$$A_z^{(m)} = A_\rho^{(m)}(z/\rho), \tag{27}$$

where $C^{(m)}$ is the weight coefficient of the $m$th term, $\zeta = \sqrt{z_r^2+D^2}$, and $z_r = z-z_s(\rho,\varphi)$. Here the function $z_s(\rho,\varphi)$, again, defines the shape of the warped current sheet.

It is not difficult to derive from (27) explicit formulae for the magnetic field components and compute from them the electric current components. Figure 9 shows the patterns of the current flow lines in the plane $z = 0$ computed from (27) for $m = 1$, 2 and 3. As can be seen, the first term with $m = 1$ yields the simplest geometry of the electric current distribution

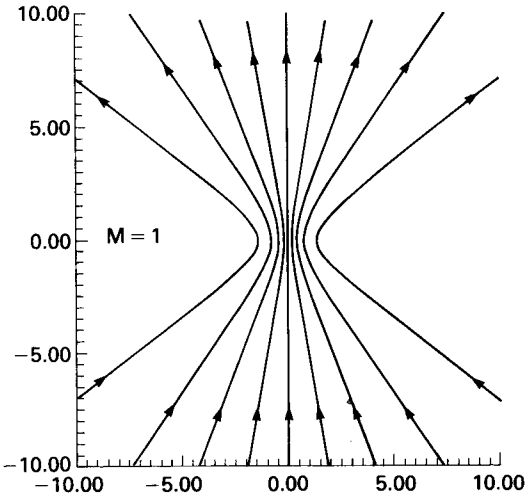


FIG. 9a. PATTERN OF THE ELECTRIC CURRENT FLOW LINES IN THE SECTORIAL CURRENT SHEET MODEL, COMPUTED FROM THE VECTOR POTENTIAL (27).
The above pattern corresponds to the first harmonic ($m = 1$).

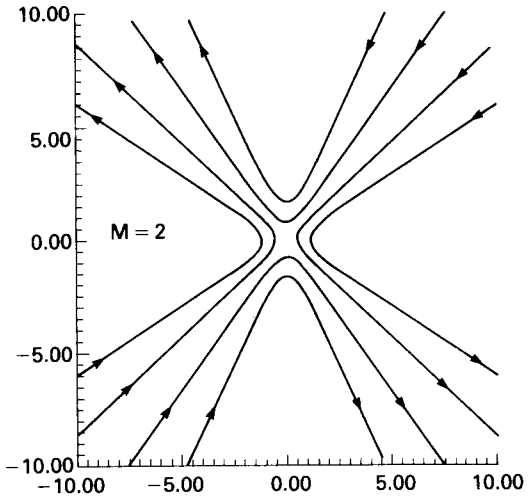


FIG. 9b. SAME AS FIG. 9a, EXCEPT FOR $m = 2$.

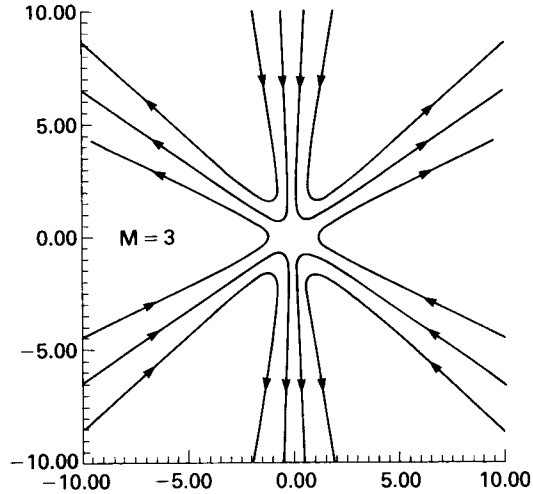


FIG. 9c. SAME AS FIG. 9a, EXCEPT FOR $m = 3$.

in which the lines converge towards the origin as a single bundle. In the case of $m = 2$ we obtain two antiparallel bundles which interconnect near the origin, and in the case of $m = 3$ the pattern is still more complex. Having composed linear combinations of the terms with various weight coefficients $C^{(m)}$ we can obtain a variety of net configurations. An appropriate choice of the function $z_s(\rho,\varphi)$ can yield the necessary shape of the current layer for modeling the

northern and southern halves of Birkeland current surface.

As a closing remark, note that the models outlined in this section are developed from planar current sheets and therefore yield inaccurate results at small geocentric distances, where we have to make the strongest deformation of the initial current layer leading to a significant secondary electric current density. For this reason, the model described in Section 4.1 would be most convenient for simulating the magnetic effects of Birkeland current jets confined within a limited interval of longitudes, such as the polar cusp currents (Iijima and Potemra, 1976b). The approach outlined in Section 4.2 can be applied for local modeling of field-aligned currents flowing along the warped boundary layer plasma sheet in the magnetotail.

## 5. CONCLUSIONS

In the present paper we have proposed methods for quantitative representation of the magnetic field from the most large-scale system I of Birkeland currents. The best results are obtained in the model which is developed by using a coordinate deformation in the expressions for the vector potential corresponding to the conical current layer of finite thickness. The model is sufficiently flexible, which allows the simulation of the main observed features of system I, which are:

(1) At ionospheric level the latitude of the field-aligned current layer depends on local time, so that by choosing proper values of parameters we can obtain a good fit to the spacecraft data (e.g. Iijima and Potemra, 1976a).

(2) Depending upon how detailed a representation of the magnetic field the model must provide (this depends also on the amount of available experimental information), we can set an appropriate number of terms in the Fourier expansions for the magnetic field components which define the local time distribution of Birkeland current magnitude.

(3) The model accounts for all the general features of the system I configuration: at relatively small altitudes the current is flowing nearly along the dipolar magnetic field lines; at larger distances they enter either the region adjacent to the polar cusps and the low-latitude boundary layer at the dayside, or extend along the plasma sheet boundary layer in the magnetotail.

(4) The model allows the incorporation of dawn–dusk asymmetry effects as well as a non-zero net current inflow in one of the hemispheres with the corresponding outflow in the opposite one; this possibility can be presumed in relation to the reconnection effects due to the $B_y$-component of the IMF.

(5) The model simulates principal anticipated effects of the geodipole tilt, namely (i) a general deformation of the current layers in both hemispheres and (ii) the North–South asymmetry in the net magnitude and M.L.T. distribution of Birkeland current intensity.

To our knowledge, the proposed model is the first attempt to develop a detailed and realistic quantitative representation of the magnetic field of Birkeland currents in a wide range of geocentric distances. The proposed model can be used for determination of main characteristics of Birkeland current system in relation to the state of the magnetosphere and the solar wind, on condition that a sufficient amount of spacecraft data taken at different altitudes are available for the statistical modeling study.

Two other methods for modeling warped current layers with variable geometry and electric current distribution have been outlined.

As a closing remark, note that we still have no suitable representation for the system II magnetic effects. The present model does not allow for a natural incorporation of the partial ring current which closes the outer bundles of the electric current flow lines. The development of such a model remains an urgent task to be solved.

*Acknowledgement*—I thank Drs D. P. Stern and W. J. Burke for discussions and critical comments.

## REFERENCES

Bateman, H. and Erdelyi, A. (1954) *Tables of Integral Transforms*. McGraw-Hill, Maidenhead.

Birkeland, K. K. (1908) *The Norwegian Aurora Polaris Expedition* 1902–1903, Vol. 1. H. Aschehoug, Chistiania, Norway.

Bythrow, P. F., Potemra, T. A. and Zanetti, L. J. (1983) Variation of the auroral Birkeland current pattern associated with the North–South component of the IMF, in *Magnetospheric currents*, *Geophys. Monograph Series*, Vol. 28, p. 131.

Crooker, N. U. and Siscoe, G. L. (1981) Birkeland currents as the cause of the low-latitude asymmetric disturbance field. *J. geophys. Res.* **86**, 11201.

Fujii, R., Iijima, T., Potemra, T. A. and Sugiura, M. (1981) Seasonal dependence of large-scale Birkeland currents. *Geophys. Res. Lett.* **8**, 1103.

Fukushima, N. (1969) Equivalence in ground magnetic effect of Chapman–Vestine's and Birkeland Alfvén's electric current systems for polar magnetic storms. *Rep. Ionosph. Space Res. Japan* **23**, 219.

Iijima, T. and Potemra, T. A. (1976a) The amplitude distribution of field-aligned currents at northern high latitudes observed by *Triad. J. geophys. Res.* **81**, 2165.

Iijima, T. and Potemra, T. A. (1976b) Field-aligned currents in the dayside cusp observed by *Triad. J. geophys. Res.* **81**, 5971.

Kamke, E. (1959) *Differentialgleichungen. Losungsmethoden*

*und Losungen, B.I, Gewohnliche Differentialgleichungen*, Part 3, Leipzig.

Kelly, T. J., Russell, C. T., Walker, R. J., Parks, G. K. and Gosling, J. T. (1986) *ISEE* 1 and 2 observations of Birkeland currents in the Earth's inner magnetosphere. *J. geophys. Res.* **91**, 6945.

Korn, G. A. and Korn, T. M. (1968) *Mathematical Handbook for Scientists and Engineers*. McGraw-Hill, New York.

Leontyev, S. V. and Lyatsky, V. B. (1974) Electric field and currents connected with *Y*-component of interplanetary magnetic field. *Planet. Space Sci.* **22**, 811.

Mead, G. D. and Fairfield, D. H. (1975) A quantitative magnetospheric model derived from spacecraft magnetometer data. *J. geophys. Res.* **80**, 523.

Newell, P. T. and Meng, C.-I. (1989) Dipole tilt angle effects on the latitude of the cusp and cleft/low-latitude boundary layer. *J. geophys. Res.* **94**, 6949.

Rich, F. J., Cattell, C. A., Kelley, M. C. and Burke, W. J. (1981) Simultaneous observations of the auroral zone electrodynamics by two satellites: evidence for height variations in the topside ionosphere. *J. geophys. Res.* **86**, 8929.

Saflekos, N. A., Sheehan, R. E. and Carovillano, R. L. (1982) Global nature of field-aligned currents and their relation to auroral phenomena. *Rev. Geophys. Space Phys.* **20**, 709.

Stern, D. P. (1983) Origins of Birkeland currents. *Rev. Geophys. Space Phys.* **21**, 121.

Stern, D. P. (1987) Tail modeling in a stretched magnetosphere 1. Methods and transformations. *J. geophys. Res.* **92**, 4437.

Stern, D. P. (1989) Modeling of Birkeland currents. *IAGA Bull. No.* 53, 6th Scientific Assembly, Exeter, July–August 1989, Part C: Abstracts, Div. II and III, IDCs, p. 429.

Sugiura, M. (1975) Identifications of the polar cap boundary and the auroral belt in the high-altitude magnetosphere: a model for field-aligned currents. *J. geophys. Res.* **80**, 2057.

Sugiura, M. (1976) Field-aligned currents observed by *OGO* 5 and *TRIAD* satellites. *Ann. Geophys.* **32**, 267.

Suzuki, A. and Fukushima, N. (1984) Anti-sunward space current below the MAGSAT level during magnetic storms. *J. Geomagn. Geoelect.* **36**, 493.

Troshichev, O. A. (1982) Polar magnetic disturbances and field-aligned currents. *Space Sci. Rev.* **32**, 275.

Tsyganenko, N. A. (1987) Global quantitative models of the geomagnetic field in the cislunar magnetosphere for different disturbance levels. *Planet. Space Sci.* **35**, 1347.

Tsyganenko, N. A. (1988) Quantitative model of the system of field-aligned magnetospheric currents. *Geomagn. Aeronomy* **28**, 331.

Tsyganenko, N. A. (1989) A magnetospheric magnetic field model with a warped tail current sheet. *Planet. Space Sci.* **37**, 5.

Tsyganenko, N. A. (1990) Quantitative models of the magnetospheric magnetic field: methods and results. *Space Sci. Rev.* **54**, 75.

Tsyganenko, N. A. and Suslikov, D. G. (1982) Large-scale magnetic effects of field-aligned currents in the magnetosphere, in *Magnetospheric Researches*, No. 1, p. 60. Nauka, Moscow (in Russian).

Tsyganenko, N. A. and Usmanov, A. V. (1982) Determination of the magnetospheric current system parameters and development of experimental geomagnetic field models based on data from *IMP* and *HEOS* satellites. *Planet. Space Sci.* **30**, 985.

Zmuda, A. J. and Armstrong, J. C. (1974) The diurnal flow pattern of field-aligned currents. *J. geophys. Res.* **79**, 4611.